22-min Au decay, but it would leave open the question of the energy and the decay of the expected low-lying 3/2+ state in the same Au isotope.

The incompleteness of the experimental results given above and the unanswered questions call for additional experiments. The decay of 22-min Au^{201} can be studied more precisely and in more detail. In particular, the relative beta intensity and the possible presence of lower energy gamma rays could be found. Furthermore, shorter bombardments and more rapid chemistry might give information about an isomer in Au^{201} analogous to those occurring in the other odd-mass Au isotopes. These investigations would not only give interesting information about Au^{201}, but they would also contribute to knowledge of the puzzling level structure in Hg^{201}.

ACKNOWLEDGMENTS

We wish to thank Paul Weston who helped obtain the experimental data. We also wish to thank Dr. Palmer Dyal who carried out the chemical separations. One of us (P.E.) would like to thank Professor Seitz, and others at the University of Illinois for the hospitality extended during her visit. She would also like to thank the International Cooperation Administration and the U. S. National Academy of Sciences for arranging and supporting her visit.

PHYSICAL REVIEW VOLUME 128, NUMBER 1 OCTOBER 1, 1962

(p,n) Cross Sections of V^{51}, Cr^{52}, Cu^{63}, Cu^{65}, Ag^{107}, Ag^{109}, Cd^{111}, Cd^{114}, and La^{139} from 5 to 10.5 MeV*

J. WING AND J. R. HUIZENGA
Argonne National Laboratory, Argonne, Illinois

(Received May 18, 1962)

(p,n) cross sections were measured by the activation technique in the energy range 5 to 10.5 MeV for the target nuclides V^{51}, Cr^{52}, Cu^{63}, Cu^{65}, Ag^{107}, Ag^{109}, Cd^{111}, Cd^{114}, and La^{139}. Approximate proton reaction cross sections were obtained at energies below the $(p,2n)$ threshold by adding to the (p,n) cross sections the previously reported charged-particle-emission (p,q) cross sections. These results are compared at a few energies with volume absorption and surface absorption optical-model calculations of the proton reaction cross sections.

I. INTRODUCTION

RECENTLY several authors[1–11] have reported on measurements of proton-reaction cross sections at energies equal to or less than 11 MeV. In several of the publications,[1–9] the experimental results have been compared with theoretical-reaction cross sections given by an optical model with parameters obtained from fitting elastic scattering data. Theoretical calculations of the reaction cross sections have assumed both surface and volume absorption.

The experiments measuring the total-reaction cross section are of two basic types. One method (hereafter referred to as method 1) consists of summing all partial-reaction cross sections such as (p,xn), (p,γ) and (p,q) cross sections, where the (p,q) cross section includes all the inelastic charged-particle emission processes. This method neglects the compound-elastic scattering cross section. In a more recently developed method (hereafter referred to as method 2) the reaction cross section is measured by direct attenuation of the incident beam intensity.[9–11]

In the determination of reaction cross sections by method 1, accurate values of the individual cross sections are desired in order to keep the sum of the individual errors to a minimum. The (p,xn) cross sections reported in the literature have been determined by activation measurements and neutron counting. At proton bombarding energies where the $(p,2n)$ threshold is exceeded, the conversion of the neutron counting rate to cross section requires information on the competition between the (p,n) and $(p,2n)$ reactions. Some of the published cross-section values from the neutron counting technique are based on calculated estimates[2]

* Based on work performed under the auspices of the U. S. Atomic Energy Commission.

[1] V. Meyer and N. M. Hintz, Phys. Rev. Letters **5**, 207 (1960).
[2] R. D. Albert and L. F. Hansen, Phys. Rev. Letters **6**, 13 (1961); Phys. Rev. **123**, 1749 (1961).
[3] R. D. Albert, Phys. Rev. **115**, 925 (1959).
[4] J. Olkowsky, M. LePape, and I. Gratot, Nuclear Phys. **23**, 164 (1961).
[5] J. Benveniste, R. Booth, and A. Mitchell, Phys. Rev. **123**, 1818 (1961).
[6] H. Taketani and W. P. Alford, Phys. Rev. **125**, 291 (1962).
[7] B. W. Shore, N. S. Wall, and J. W. Irvine, Jr., Phys. Rev. **123**, 276 (1961).
[8] G. A. Jones and J. P. Schiffer, Bull. Am. Phys. Soc. **6**, 273 (1961).
[9] G. W. Greenslees and O. N. Jarvis, *Proceedings of the International Conference on Nuclear Structure* (University of Toronto Press, Toronto, 1960), p. 217.
[10] R. F. Carlson, R. M. Eisberg, R. H. Stokes, and T. H. Short, Bull. Am. Phys. Soc. **6**, 441 (1961).
[11] G. Igo and B. Wilkins, Bull. Am. Phys. Soc. **6**, 506 (1961); and (private communication).

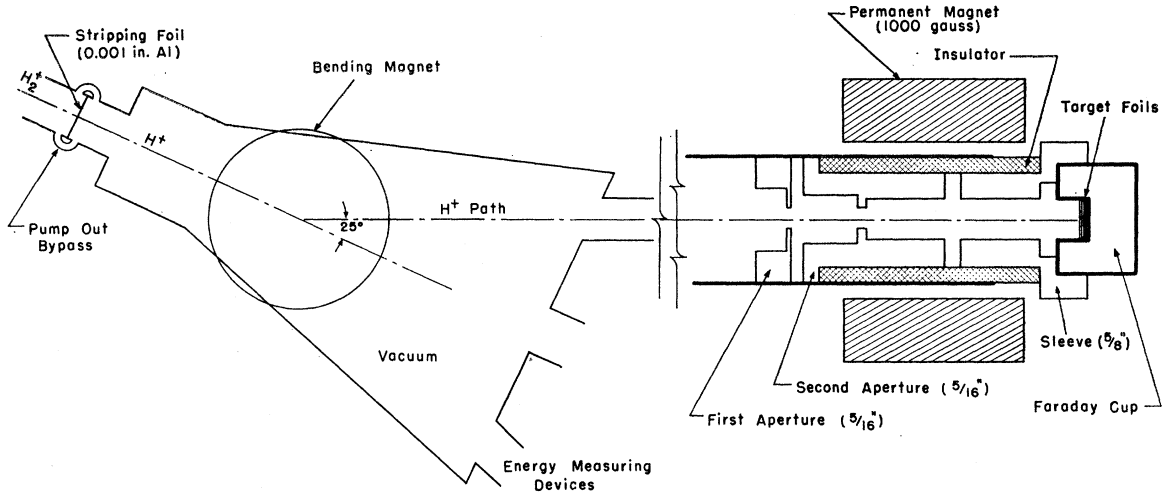

FIG. 1. Schematic diagram of target assembly (not drawn to scale) with the target holder enlarged many times at the right. Distance between apertures: $1\frac{1}{4}$ in. Second aperture to target foil distance $3\frac{1}{4}$ in.

of the (p,$2n$) competition rather than experimental results. On the other hand, cross-section measurements made by the activation technique require accurate information on the decay schemes of the residual nuclei.

The present paper reports (p,n) cross sections for several nuclei in the energy range 5 to 10.5 MeV measured by the activation technique. The targets Ag^{107}, Ag^{109}, Cd^{111}, Cd^{114}, and La^{139} were chosen because the (p,γ) and (p,q) cross sections are expected to be small in the above proton-energy range. Therefore, at energies below the (p,$2n$) threshold, the (p,n) cross sections of these nuclei give a good estimate of their total reaction cross sections.

The (p,n) cross sections of Cu^{63} and Cu^{65} were remeasured since conflicting values of these cross sections have appeared in the literature.[2] It is important to obtain reliable values of these cross sections since one of the principal justifications for a surface-absorption term in the optical model is the large value[1,2] of the total-reaction cross section reported for copper.

II. EXPERIMENTAL PROCEDURE

The (p,n) reactions were studied with the Argonne 60-in. cyclotron which accelerates molecular hydrogen to an energy of 21.3 MeV. A schematic diagram of the target assembly is shown in Fig. 1. The H_2^+ beam from the cyclotron was first passed through a 0.001-in. Al stripping foil. The resulting H^+ beam with an energy of about 10.5 MeV was passed through a bending magnet in order to separate the deuteron contamination in the primary beam. The proton beam was collimated with two apertures. A sleeve surrounded by a magnet was placed between the second aperture and the target to collect electrons which are back scattered from the target. The average current on the target was kept at 1 μA or less in most of the bombardments. A piece of filter paper which was placed behind the targets served to indicate the beam position and area. The total number of protons striking the target was measured with a Faraday cup and a vibrating reed electrometer, the output of which was fed to an integrator. Preceding every bombardment, a trial run was made with a dummy target which was insulated from the target assembly in order to make sure that the currents on the second aperture and sleeve were small and that the beam was well focused.

The mean range of the protons was measured in each experiment by the aluminum absorption technique. The measured mean ranges were converted to proton energies with the range-energy relationship of Sternheimer.[12] The emergent beam of protons (10.5 MeV) has an energy spread with a full width at half-maximum intensity of about 0.1 MeV.

The targets of V, Cr, Cu, Ag, and Cd were metallic foils of approximately 5 mg/cm^2 thickness. The La targets were prepared by volatizing lanthanum metal onto 0.0005-in. Al foils. The weights of the La targets were determined after completion of the counting by spectrographic analysis. The reduction in proton energy was accomplished by placing metallic absorbers of known thicknesses in front of the target foils. The range-energy relationships of Sternheimer[12] were used for Al, Cu, and Ag. The range-energy relationships for V and Cr were assumed to be equal to Cu and that for Cd equal to Ag. In a few runs V, Cr, Cu, and Ag foils were bombarded together in order to cross check the results (one run included La). Many of the bombardment assemblies included, in addition to the target material, a Cu foil. The Zn^{65} activity produced by the Cu^{65}(p,n)Zn^{65} reaction was used to give a direct comparison between the (p,n) cross section of Cu^{65} and the other target materials. One bombardment was made with stacked foil targets of Bi^{209} (evaporated onto Al),

[12] R. M. Sternheimer, Phys. Rev. **115**, 137 (1959).

TABLE I. Decay properties of product nuclei.

Target	Product	Half-life of product	Radiation detected	Pertinent decay scheme information[a]
V^{51}	Cr^{51}	27.8 day	325-keV γ	9% E.C. to 325-keV level; $e/\gamma=0.0015$
Cr^{52}	Mn^{52m}	21.3 min	1.43-MeV γ	99% β^+
	Mn^{52g}	5.6 day	1.43-MeV γ	65% E.C.; 35% β^+
Cu^{63}	Zn^{63}	38.3 min	β^+, 511–511 keV γ's in coincidence	93% β^+
Cu^{65}	Zn^{65}	245 day	1.12-MeV γ	49% of the total disintegration decay to 1.12-MeV level;[b] $e/\gamma=2\times10^{-4}$
Ag^{107}	Cd^{107}	6.7 h	95-keV γ	>99% E.C. to 95-keV level; $\alpha_K=9.5$; $K/(L+M)=0.88$; $e/\gamma=20.3$
Ag^{109}	Cd^{109}	470 day	88-keV γ	100% E.C. to 88-keV level; $\alpha_K=10.3$; $K/(L+M)=0.84$; $e/\gamma=22.5$
Cd^{111}	In^{111}	2.81 day	247-keV γ	100% E.C. to 247-keV level; $\alpha_K=0.054$; $K:L:M=59:10:2$
Cd^{114}	In^{114m}	50.0 day	β^- of In^{114g}	96.5% I.T. to In^{114g}
Cd^{114}	In^{114g}	72 sec	β^-	98% β^-
La^{139}	Ce^{139}	140 day	166-keV γ	100% E.C. to 166-keV level; $\alpha_K=0.22$; $K/(L+M+N)=5.7$

[a] See reference 14.
[b] This value is based on the measured value of the (K capture to 1.12-MeV level/total K capture) ratio of 0.50 ± 0.02, 1.7% positron branch, and the assumption that the (K-electron capture/total electron capture) ratios for the ground and excited state decay are equal.

Ag, and Cu in order to check previously measured cross sections[13] of Bi^{209} and to compare the cross sections of these targets.

The (p,n) cross sections were determined by an absolute measurement of the disintegration rates of the reaction products. The foils were counted without radiochemical separation since interfering activities were negligible. The loss of reaction products by recoil was very small in our experimental arrangement and neglected in the computation of the cross sections. In most of the measurements a characteristic gamma ray of the reaction product was counted, and in many cases the activity further identified by a half-life determination. The principal features of the decay schemes[14] of the reaction product nuclei are summarized in Table I. The characteristic radiations which were counted for each nuclide are also listed in Table I.

The photopeak intensities of the various gamma rays were measured with a 3-×3-in. NaI(Tl) crystal and a 256-channel pulse-height analyzer. The product of the absolute crystal efficiency and the photopeak-to-total ratio for each of the different gamma rays was obtained from the compilations of Heath[15] and Lazar.[16] Corrections were made for the escape-peak probability, self-absorption in the target foil, and absorption in the detector window, although these corrections were small in all cases.

An independent calibration of our detector arrangement was made for 1.12-MeV gamma rays [gamma rays of this energy were detected for Zn^{65} produced in the $Cu^{65}(p,n)Zn^{65}$ reaction]. The disintegration rate of a Sc^{46} sample was determined by counting its beta particles in a 4π gas-flow proportional counter. By utilizing the known decay scheme[14] of Sc^{46} (approximately one 1.12-MeV γ ray/dis), the photopeak detection efficiency of the 1.12-MeV γ rays was directly established. This measured efficiency was in good agreement with the value determined from the above compilations.

The β^+ and β^- activities of Zn^{63} and In^{114}, respectively, were counted in a gas-flow proportional counter. In the determination of the yield of Zn^{63} for a number of the bombardments, a second counting technique was employed. The two 511-keV γ rays resulting from the annihilation of the positrons were detected in $2\frac{1}{2}$-×$2\frac{1}{4}$-in. and 3-×3-in. NaI(Tl) crystals, and analyzed and recorded by a coincidence counter. Single-channel analyzers were used to select the annihilation radiations, and the pulses from coincident events were added and fed to a discriminator which triggered for sum pulses above a fixed energy. The counting efficiency of this counter for positrons was calibrated with a Na^{22} standard. The counting efficiency of the proportional counter for the positrons of Zn^{63} was determined from the coincidence counting of the 511-keV annihilation gamma rays of Zn^{63}. The counting efficiency of the β^- particles of In^{114} was established with Y^{90} and P^{32} standards.

III. (p,n) CROSS SECTIONS

Our experimental values of the (p,n) cross sections for target nuclides V^{51}, Cr^{52}, Cu^{63}, Cu^{65}, Ag^{107}, Ag^{109}, Cd^{111}, Cd^{114}, La^{139}, and Bi^{209} bombarded with protons of energy between 5 and 10.5 MeV are summarized in Table II. These (p,n) cross-section values along with values from other experimenters are plotted as a function of proton energy in the laboratory system in Figs. 2 to 10. In the figures, the experimental techniques

[13] C. G. Andre, J. R. Huizenga, J. F. Mech, W. J. Ramler, E. G. Rauh, and S. R. Rocklin, Phys. Rev. **101**, 645 (1956).
[14] Nuclear Data Sheets, National Academy of Sciences (National Research Council, Washington, D. C., 1960); Strominger, Hollander, and Seaborg, Revs. Modern Phys. **30**, 585 (1958).
[15] R. L. Heath, Atomic Energy Commission Report IDO-16408, 1957 (unpublished).
[16] N. H. Lazar, Trans. IRE NS-5, No. 3, 138 (1958).

TABLE II. Experimental (p,n) cross sections (σ in millibarns) as a function of proton bombarding energy (MeV) in the laboratory system.

$V^{51}(p,n)Cr^{51}$		$Cr^{52}(p,n)Mn^{52}$			$Cu^{63}(p,n)Zn^{63}$		$Cu^{65}(p,n)Zn^{65}$		$Ag^{107}(p,n)Cd^{107}$		$Ag^{109}(p,n)Cd^{109}$		$Cd^{111}(p,n)In^{111}$		$Cd^{114}(p,n)In^{114}$			$La^{139}(p,n)Ce^{139}$		$Bi^{209}(p,n)Po^{209}$	
E_p	σ	E_p	$\sigma_{Mn^{52m}}$	$\sigma_{Mn^{52g}}$	E_p	σ	E_p	σ	E_p	σ	E_p	σ	E_p	σ	E_p	$\sigma_{In^{114m}}$	$\sigma_{In^{114g}}$	E_p	σ	E_p	σ
10.4	645	10.5	370	98	10.5	443	10.5	751, 760, 735	10.5	581	10.5	305	10.1	540	10.3	347		10.3	301	10.3	114
10.1	650, 623	10.1	365	88	10.3	423	10.4	760	10.45	589	10.4	305	9.75	526	10.1	340		10.2	293	9.78	90
9.93	632	9.9	326	79	10.1	440	10.3	722	10.43	590	10.2	320	9.5	508	10.0		264	9.1	197		
9.6	632	9.2	350	69	9.92	420, 392	10.2	762	10.35	576	9.85	342	8.4	366	9.9		275	7.4	66		
9.5	631	9.1	344	84	9.9	405, 402	10.1	707, 696	10.33	562	9.4	353	7.4	262	9.75	321		6.6	33		
8.65	596	9.0	288	65	9.85	407	9.9	716, 710, 723	10.16	521	9.1	362	6.4	134	9.6	328		6.0	16		
8.0	578	8.9	296	60	9.83	390, 391	9.85	718	9.85	521	8.9	365	5.4	45	9.5	308		5.2	4		
7.7	559	8.4	281	51	9.6	399	9.83	732, 712	9.45	489	8.7	332	4.4	12	8.9		268	4.5	0.2		
7.0	544	8.0	250	44	8.9	377	9.8	728	9.0	440, 421	8.0	280	3.3	0.9	8.4	201					
6.65	515	8.0	260	41	8.87	377	9.6	676, 673, 692	8.9	418	6.9	146	2.1	<0.04	8.4	215					
5.65	430	7.4	224	31	8.6	360	9.45	689	8.7	375	6.5	130			7.8		228				
5.0	351	7.0	220	23	7.7	320	9.0	624, 630	8.1	324	6.0	95			7.8		215				
4.7	286	7.0	210	23	7.6	313	8.9	652	8.0	296	5.0	32, 24			7.5	135					
3.7	145	6.4	158	11	6.8	268	8.87	648	7.1	209					7.4	119					
3.1	34	6.0	28	1.1	6.6	248	8.8	615	6.9	179					6.8		172				
		5.9	20	1.3	6.4	237	8.62	617	6.4	133					6.8		140				
		5.8	7.7	0.4	5.6	184, 187	8.6	578	6.1	115					6.4	54					
		5.8	4.2	0.2	4.5	55	8.4	629	6.0	98					6.3	57					
							8.1	560	5.1	38					5.9		94				
							7.9	528	5.0	24					5.8		91				
							7.73	572	4.9	19					5.4	15					
							7.6	518	3.2	0.5					5.2	14					
							7.4	535	1.9	0.06					4.7		26				
							7.3	550							4.4	3					
							6.8	420													
							6.6	430													
							6.5	428													
							6.2	390													
							6.0	361													
							5.6	341													
							5.5	317													
							5.1	306													
							4.5	175													

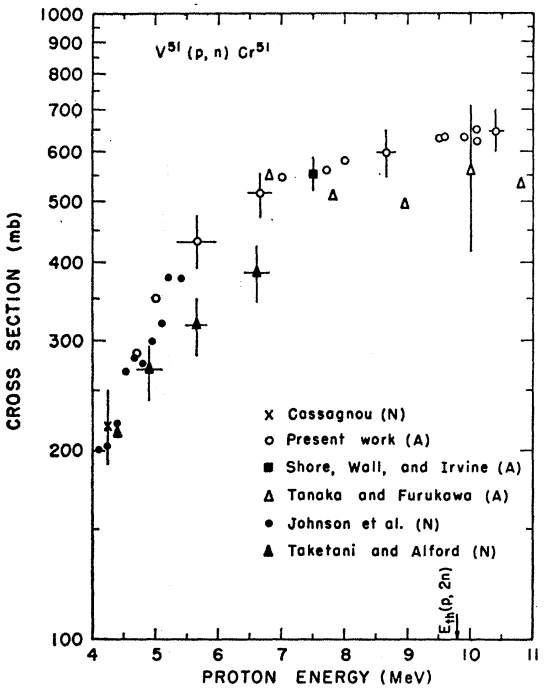

FIG. 2. Excitation function of $V^{51}(p,n)Cr^{51}$. The proton energy is in the laboratory scale.

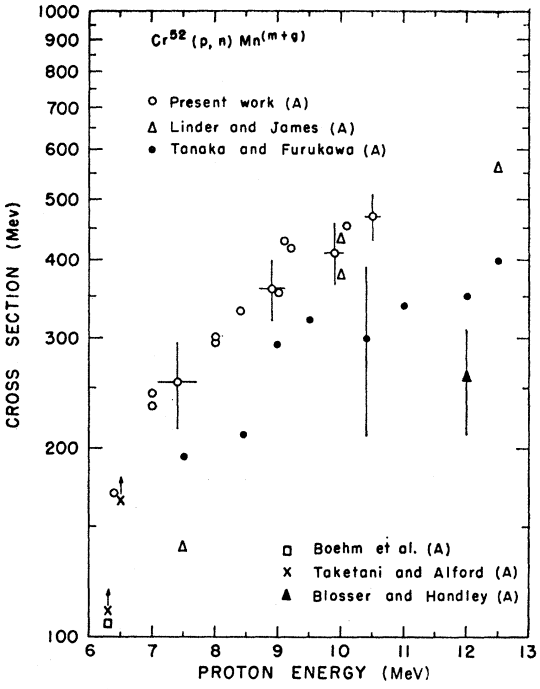

FIG. 4. Excitation function of $Cr^{52}(p,n)Mn^{52(m+g)}$.

of activation analysis and neutron counting are designated by (A) and (N), respectively. The (p,$2n$) threshold energies are indicated on the figures by labeled arrows.

The estimated experimental errors in the (p,n) cross sections are included in Figs. 2 to 10 for selected proton energies. The sources of error include uncertainties in the integrated beam currents, target weights, counting

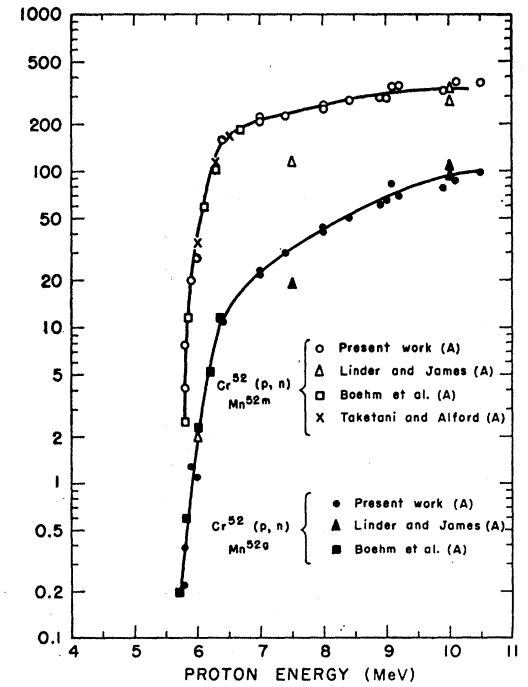

FIG. 3. Excitation functions of $Cr^{52}(p,n)Mn^{52m}$ and $Cr^{52}(p,n)Mn^{52g}$.

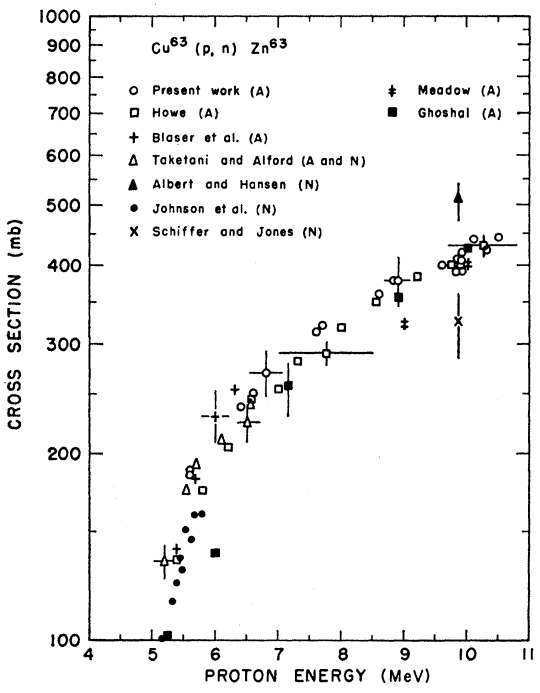

FIG. 5. Excitation function of $Cu^{63}(p,n)Zn^{63}$. See the note added in proof at the end of Sec. III.

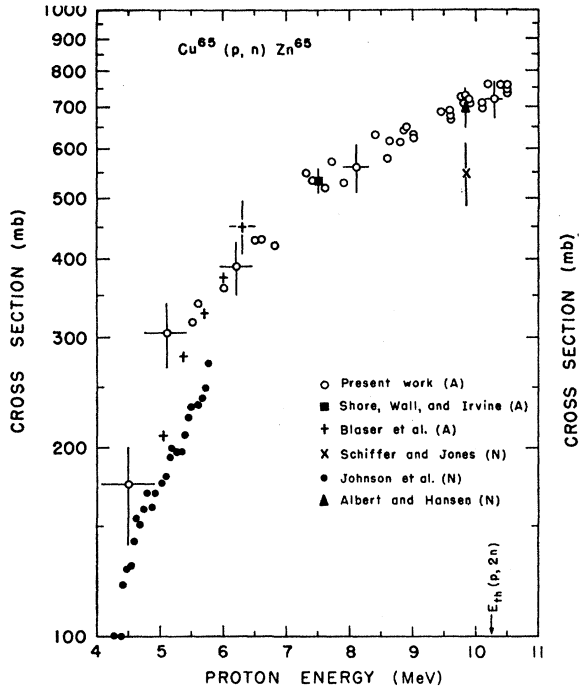

FIG. 6. Excitation function of $Cu^{65}(p,n)Zn^{65}$.

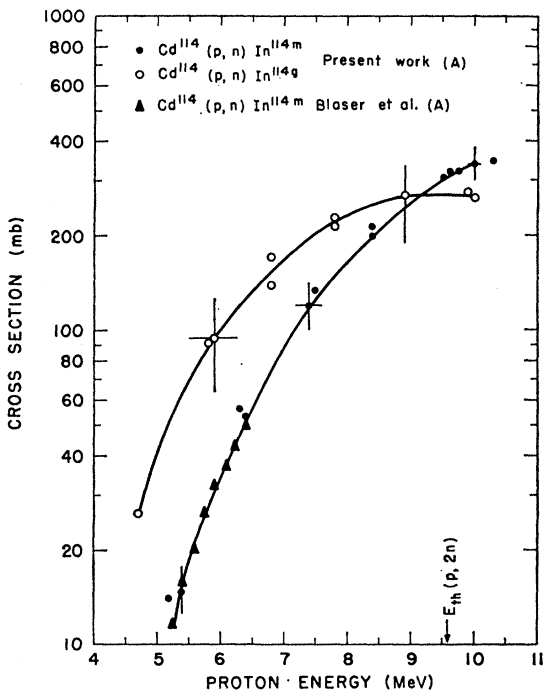

FIG. 8. Excitation functions of $Cd^{114}(p,n)In^{114m}$ and $Cd^{114}(p,n)In^{114g}$.

efficiencies, counting statistics, conversion coefficients, decay branching ratios, and half-life values. The total error in the cross sections are thought to be 10% or less for most of the targets. The uncertainty in the proton energy at 10 MeV is about 0.15 MeV and increases to approximately 0.5 MeV at 5 MeV.

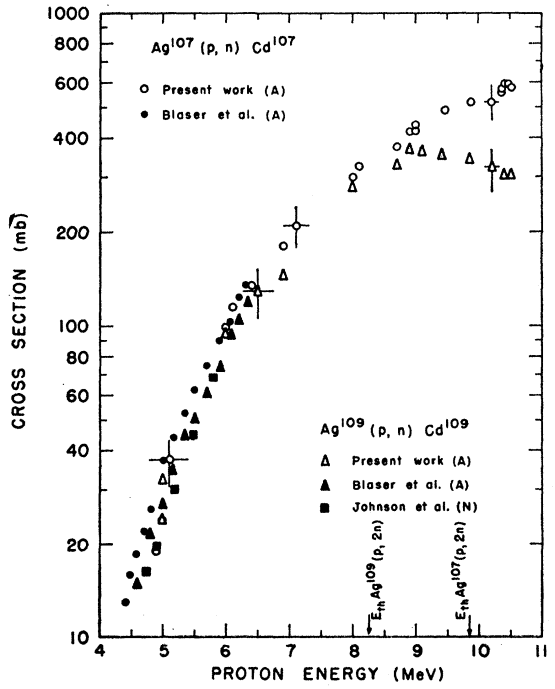

FIG. 7. Excitation functions of $Ag^{107}(p,n)Cd^{107}$ and $Ag^{109}(p,n)$ Cd^{109}.

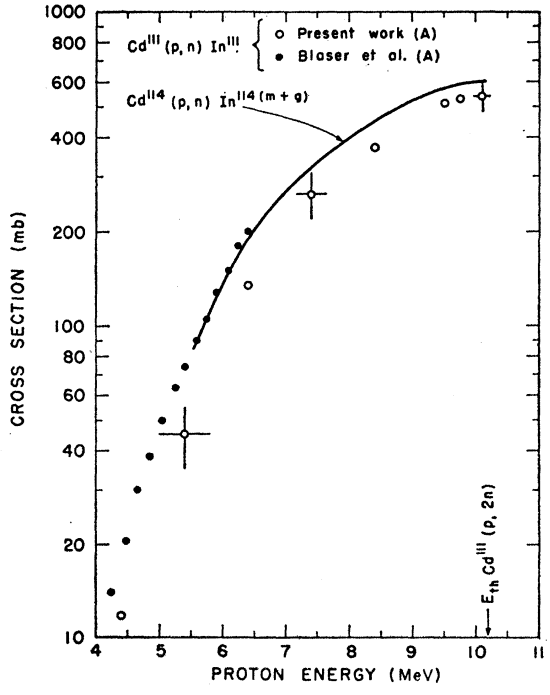

FIG. 9. Excitation functions of $Cd^{114}(p,n)In^{114(m+g)}$ and $Cd^{111}(p,n)In^{111}$.

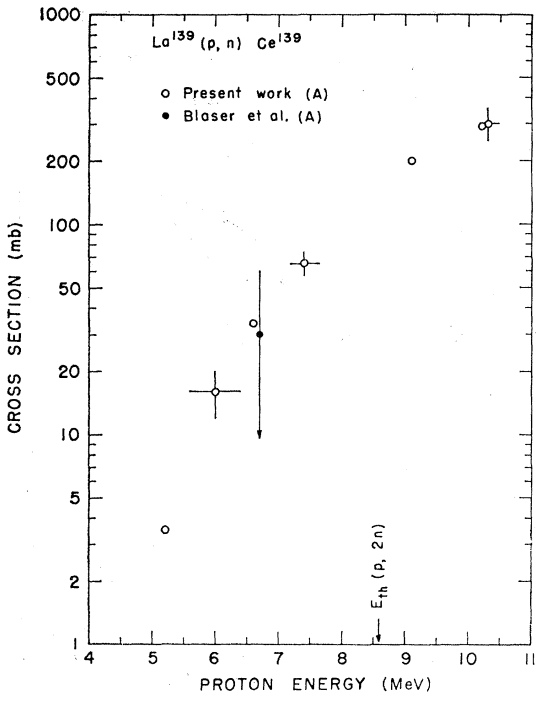

FIG. 10. Excitation function of $La^{139}(p,n)Ce^{139}$.

The experimental methods used by other investigators[2,6–8,17–25] whose results are included in Figs. 2 to 10 are briefly described in Table III. For those cases in which new decay-scheme data have become available, thee xperimental values of other workers were multiplied by an appropriate factor to correct for the newer data. A qualitative measure of the agreement of the various experimenters is indicated in column 6 of Table III, and a more quantitative measure of the agreement can be seen in the various figures. Some of the cross section measurements of other investigators (see Table III) were made with protons which were degraded in energy by a large factor with absorbers and, hence, subject to considerable uncertainty in energy.

Several groups[2,8] have determined the (p,n) cross sections of Cu^{63} and Cu^{65} with protons of approximately 10 MeV. The results of Jones and Schiffer[8] for both copper isotopes are approximately 20% smaller than our results. The cross section for Cu^{65} measured by Albert and Hansen[2] agrees with our value,[25a] whereas their cross section of Cu^{63} is about 20% larger than our value. The disagreement between our results and those of Jones and Schiffer may be due to a calibration error since their cross-section ratio of the copper isotopes agrees with ours. However, the value of this ratio determined by Albert and Hansen is in disagreement with our and Jones and Schiffer's values. Since Albert *et al.* and Jones *et al.* were both counting neutrons, the large discrepancy in the cross section ratio of the copper isotopes by these two groups is difficult to understand.

Note added in proof. In a private communication from L. F. Hansen, we have learned that Albert and Hansen have reduced their $Cu^{63}(p,n)$ cross section with 10-MeV protons to 450 mb in good agreement with our value. This, of course, makes all the above cross section ratios agree.

IV. TOTAL PROTON REACTION CROSS SECTIONS

In order to obtain the total reaction cross sections for protons (by method 1) from the (p,n) cross sections, one must add the values of the partial-reaction cross sections for all other processes which are energetically possible. Therefore, in addition to the (p,n) cross sections, it may be necessary to have information on the cross sections of the $(p,2n)$, (p,γ), and (p,q) reactions in order to derive a reasonably accurate estimate of the total-reaction cross section. The (p,q) cross sections include all the inelastic charged-particle emission processes. This method of measuring the total-reaction cross section neglects the compound-elastic scattering cross section. The (p,γ) cross sections are usually relatively small at excitation energies a few MeV above the threshold for particle emission and are neglected.

The (p,q) cross sections of Cu^{63} and Cu^{65} have been measured[1,5,7] for the proton-energy range covered in these experiments. The $(p,2n)$ thresholds of Cu^{63} and Cu^{65} are large enough to prohibit a contribution of these reactions for protons of less than 10.5 MeV. The (p,q) cross sections from the literature[1,5,7] are plotted as a function of proton energy in Fig. 11. These (p,q) cross sections are summed with our (p,n) cross sections, and the resulting values of the total-reaction cross section are plotted as a function of proton energy in the laboratory scale in Fig. 11. The total cross sections of Cu^{65} are about 60 mb larger than those of Cu^{63} at equal proton energies between 6 and 10.5 MeV, although within the experimental errors the total-reaction cross sections of the two copper isotopes are in agreement. The total-reaction cross sections of copper measured by the beam attenuation technique (method 2) by three different groups,[9–11] each at a single energy, are also plotted in Fig. 11. The revised datum of Igo and Wilkins

[17] S. Tanaka and M. Furukawa, J. Phys. Soc. (Japan) **14**, 1269 (1959).
[18] C. H. Johnson, A. Galonsky, and C. N. Innskeep, U. S. Atomic Energy Commission Report ORNL-2910, 1960 (unpublished).
[19] B. Linder and R. A. James, Phys. Rev. **114**, 322 (1959).
[20] F. Boehm, P. Marmier, and P. Preiswerk, Helv. Phys. Acta **25**, 599 (1952).
[21] H. G. Blosser and T. H. Handley, Phys. Rev. **100**, 1340 (1955).
[22] J.-P. Blaser, F. Boehm, P. Marmier and D. C. Peaslee, Helv. Phys. Acta **24**, 3 (1951); J.-P. Blaser, F. Boehm, P. Marmier, and P. Scherrer, *ibid.* **24**, 441 (1951).
[23] H. A. Howe, Phys. Rev. **109**, 2083 (1958).
[24] S. N. Ghoshal, Phys. Rev. **80**, 939 (1950).
[25] J. W. Meadows, Phys. Rev. **91**, 885 (1953).

[25a] Our value of the $Cu^{65}(p,n)$ cross section reported in the Bull. Am. Phys. Soc. **6**, 260 (1961) is incorrect due to an erroneous calibration factor. However, our present value was reported at the meeting.

TABLE III. Summary of pertinent information used in the determination of (p,n) cross sections by other investigators.

Target	Author identification	Initial proton energy (MeV)	Method of determination of cross section	Conversion factor[a]	Results relative to ours	Reference
V^{51}	Shore	7.5	Scintillation counting, calibrated by x-ray–γ-ray coincidence counting of Cr^{51}. Current measured by Faraday cup.	1	Same	7
	Tanaka	14	NaI scintillation counting of 0.32-MeV γ. Current measured by Faraday cup.	1	Same	17
	Taketani	Variable	Neutron counting by BF_3 counter, relative to his $Cu^{63}(p,n)Zn^{63}$ results.	1	Low	6
	Johnson	Variable	Neutron counting by 4π graphite sphere detector.	1	Same	18
	Cassagnou		Neutron counting	1	Same	[b]
Cr^{52}	Linder	21	Scintillation counting of positron annihilation radiations by NaI, relative to his and Ghoshal's (reference 24) $Cu^{63}(p,n)Zn^{63}$ results.	85 /93	Same	19
	Taketani	Variable	Coincidence counting of positron annihilation radiations by NaI, calibrated by NBS[c] Na^{22} standard. Current measured by Faraday cup.	1	Same	6
	Tanaka	14	Mn^{52m}/Mn^{52g} by NaI scintillation counting of 1.45-MeV γ; (d/m) of Mn^{52} by γ-γ coincidence counting; relative yield of Mn^{52} by counting γ rays >0.6 MeV. Current measured by Faraday cup.	1	Same	17
	Boehm	6.5	(Not given but presumably Geiger counting of positrons.)	1	Same	20
	Blosser	22	Geiger counting of positrons, relative to Ghoshal's $Cu^{63}(p,n)Zn^{63}$ cross section at 12 MeV.	85 /93	"Low"	21
Cu^{63}	Blaser	6.5	Geiger counting of positrons, calibrated by NBS $Ra(D+E)$ standard.[c] Current measured by Faraday cup.	85 /93	Same	22
	Howe	20	Coincidence counting of positron annihilation radiations by NaI, calibrated by NBS Na^{22} standard. Current measured by Faraday cup.	89.3/93	Same	23
	Ghoshal	32	Counting positrons, assuming 85% β^+ branching. Current measured by Faraday cup.	85 /93	Same	24
	Meadows	100	Geiger counting of positrons. Current monitored by $Al^{27}(p,3pn)Na^{24}$ cross sections which were calibrated by $C^{12}(p,pn)C^{11}$ cross sections.	1	Same	25
	Albert	9.85	Neutron counting by BF_3 counter.	1	High	2
	Johnson	Variable	Neutron counting by 4π graphite sphere detector.	1	Same	18
	Schiffer	9.85	Neutron counting by BF_3 counter.	1	Low	8
	Taketani	Variable	Coincidence counting of positron annihilation radiations by NaI and neutron counting by BF_3 counters.	1	Same	6
Cu^{65}	Shore	7.5	Scintillation counting, calibrated by x-ray–γ-ray coincidence counting of Zn^{65} source, NBS's Zn^{65} and Mn^{54} sources. Current measured by Faraday cup.	1	Same	7
	Blaser	6.5	Geiger counting of positrons and γ-rays; 46% E.C. to the 1.12-MeV state, 54% E.C. to ground state, 2.2% β^+. Current measured by Faraday cup.	45 /49	Same	22
	Albert	9.85	Neutron counting by BF_3 counter.	1	Same	2
	Johnson	Variable	Neutron counting by 4π graphite sphere detector.	1	Low	18
	Schiffer	9.85	Neutron counting by BF_3 counter.	1	Low	8
Ag^{107}	Blaser	6.5	Geiger counting of K x rays; $e/\gamma=16\pm3$. Current measured by Faraday cup.	21.3/17	Same	22
Ag^{109}	Blaser	6.5	Geiger counting of K x rays; $e/\gamma=19\pm3$. Current measured by Faraday cup.	23.5/20	Same	22
	Johnson	Variable	Neutron counting by 4π graphite sphere detector.	1	Same	18
Cd^{111}	Blaser	6.5	Geiger counting of γ rays and conversion electrons. Current measured by Faraday cup.	1	High	22
Cd^{114}	Blaser	6.5	Geiger counting of 1.98-MeV β^- of In^{114g}, calibrated by NBS Na^{22} standard. Current measured by Faraday cup. Assuming 100% I.T. and 97% β^- decay of In^{114g}.	1.025	Same	22
La^{139}	Blaser	6.5	Geiger counting of γ rays, calibrated by $Ra(D+E)$ and Co^{60} standards of NBS; assumed 1 γ per disintegration of Ce^{139}. Current measured by Faraday cup.	1.26	Same	22

[a] A factor used to convert the results for comparison with our data on the same basis of decay scheme. For example: Linder's Cr^{52} data, determined relative to Ghoshal's Cu^{63} results (which were based on 85% β^+ branching of Zn^{63}), must be multiplied by 85/93, because we used 93% β^+ for Zn^{63} decay.
[b] Y. Cassagnou, J. M. F. Jeronymo, C. Levi, L. Papineau, and D. Stanojevic, J. phys. radium 22, 604 (1961).
[c] See National Bureau of Standards Circular No. 594 (Superintendent of Documents, U. S. Government Printing Office, Washington D. C., 1958).

at 10.1 MeV agrees with the data determined by method 1.

The (p,q) cross sections of V^{51} are >165 mb[1] and 134 mb[7] at proton energies of 9.85 and 7.5 MeV, respectively. By adding these values to our (p,n) cross sections at corresponding energies, we derive cross sections of >800 mb and 690 mb for 9.85- and 7.5-MeV protons, respectively. The value at 7.5-MeV proton energy is in excellent agreement with that of Shore, Wall, and Irvine.[7] This is a result of our agreement on

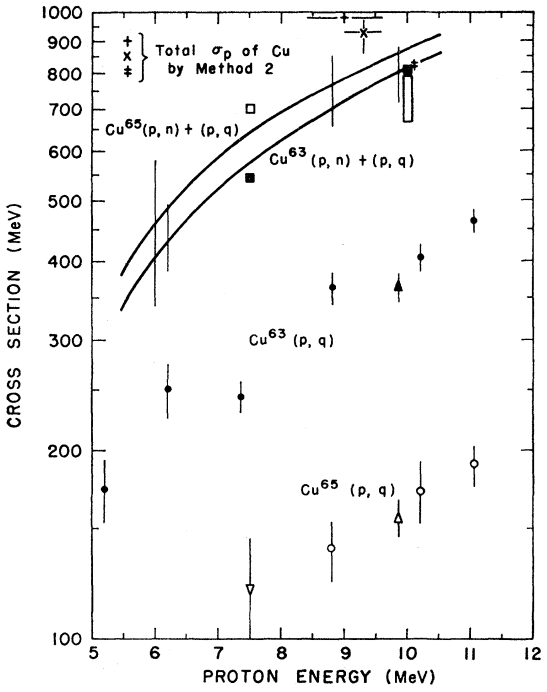

FIG. 11. Total proton reaction and (p,q) cross sections of Cu. Open circles and triangles represent $Cu^{65}(p,q)$ cross sections; solid circles and triangles represent $Cu^{63}(p,q)$ cross sections. Solid curves and the symbols +, ×, and ≠, represent total proton-reaction cross sections. The data represented by the symbols ○ and ● are from Benveniste *et al.* (reference 5), △ and ▲ from Meyer and Hintz (reference 1), ▽ from Shore *et al.* (reference 7), × from Greenslees and Jarvis (reference 9), + from Carlson *et al.* (reference 10), and ≠ from Igo and Wilkins (reference 11). The symbols ■ and □ represent theoretical-reaction cross sections calculated with surface and volume absorption, respectively. ■ and □ at 7.5 MeV are from reference 7, ■ at 10 MeV from references 29 and 2, and □ at 10 MeV from references 27 and 28. *Note added in proof.* The reaction cross section of copper measured at 9 MeV by R. F. Carlson, R. M. Eisberg, R. H. Stokes, and T. H. Short [Nuclear Phys. **36**, 511 (1962)] has been revised downward to 895±80 mb.

the $V^{51}(p,n)$ cross section with 7.5-MeV protons. The $V^{51}(p,p')$ cross sections of Seward[26] were added to our (p,n) cross sections at proton energies less than 6.5 MeV. At the lower energies it was assumed that the other (p,q) cross sections were negligible. The resulting total reaction cross sections of V^{51} are plotted in Fig. 12.

Cross sections for the (p,q) reactions in Cr^{52}, Ag^{107}, Ag^{109}, Cd^{111}, Cd^{114}, and La^{139} targets are not available. These cross sections are expected to be small for the latter five targets due to the large Coulomb barriers of these nuclei relative to copper and vanadium. This assumption is supported by measured values of about 30 mb for the (p,q) cross sections[1] of natural silver and tin bombarded with 10-MeV protons. The (p,n) cross sections of Ag^{107}, Ag^{109}, Cd^{111}, Cd^{114}, and La^{139} are probably therefore good estimates of the total-reaction cross sections of these nuclei at proton energies less than the $(p,2n)$ thresholds. The reaction cross sections for silver, cadmium, lanthanum, and bismuth[13] which are plotted in Fig. 13 are based on the above assumption, and, hence, do not contain a correction for the (p,q) cross section.

V. OPTICAL MODEL CALCULATIONS

With a computer code based on the optical model with only volume absorption[27] and using the same Woods-Saxon form factor for the real and imaginary parts of the nuclear potential, some sample calculations have been made to investigate the sensitivity of the total-reaction cross section of copper with 10-MeV protons to the various parameters. Using the parameters for Cu obtained by Glassgold for elastic scattering data, we varied r_0 and V. The results indicate that effects of size resonance are appreciable. If one replaces W with a smaller absolute value than −8.6 MeV used by Glassgold, these size resonances become much more pronounced. These results are shown in Figs. 14(a) and 14(b). Thus, it seems that changing the parameters increases or decreases the value of the reaction cross section and also that the sensitivity to the parameters is going to be a function of the location on the size

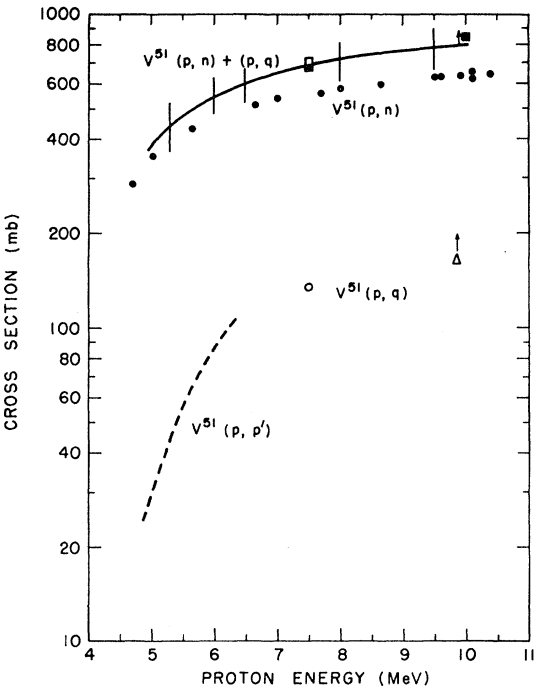

FIG. 12. Total proton reaction and (p,q) cross section of V^{51}. Solid curve represents the total proton cross sections; ●, the (p,n) cross sections; ○, the (p,q) cross section of Shore, *et al.* (reference 7); △, the (p,q) cross section of Meyer and Hintz (reference 1); and dashed curve represents the (p,p') cross sections of Seward (reference 26). The symbols ■ and □ represent the theoretical-reaction cross sections with surface and volume absorption, respectively. ■ and □ at 7.5 MeV are from reference 7, and ■ at 10 MeV from references 29 and 2.

[26] F. D. Seward, Atomic Energy Commission Report NYO-2267 (unpublished); also see reference 6.

[27] A. E. Glassgold, W. B. Cheston, M. L. Stein, S. B. Schuldt, and G. W. Erickson, Phys. Rev. **106**, 1207 (1957).

resonance. The dependence of the total-reaction cross section on W for two choices of the location on the size resonance is illustrated in Fig. 14(c). Glassgold[27] and Nodvik and Saxon[28] give permissible limits with respect to variations in V and r_0, but it is not clear to what extent W can be varied without seriously disturbing the agreement with elastic scattering data. From the calculations of Glassgold[27] and Nodvik and Saxon[28] (who included a spin-orbit term) the total-reaction cross section for copper is bounded by the values 670 mb ($r_0=1.20$ F) and 800 mb ($r_0=1.33$ F). As already pointed out by others, the experimental 10-MeV cross sections for copper are slightly larger than the values based on optical-model calculations with previous parameters and uniform nuclear volume absorption. The average of our reaction cross sections of Cu^{63} and Cu^{65} with 10-MeV protons is 850 mb, in good agreement with the average of the results reported by Albert and Hansen,[2] and the value of 820 mb reported by Igo and Wilkins.[11]

Optical-model calculations of the reaction cross sections with surface absorption have been made by Bjorklund and Fernbach[29] and reported by Albert and Hansen.[2] The calculations were performed with values

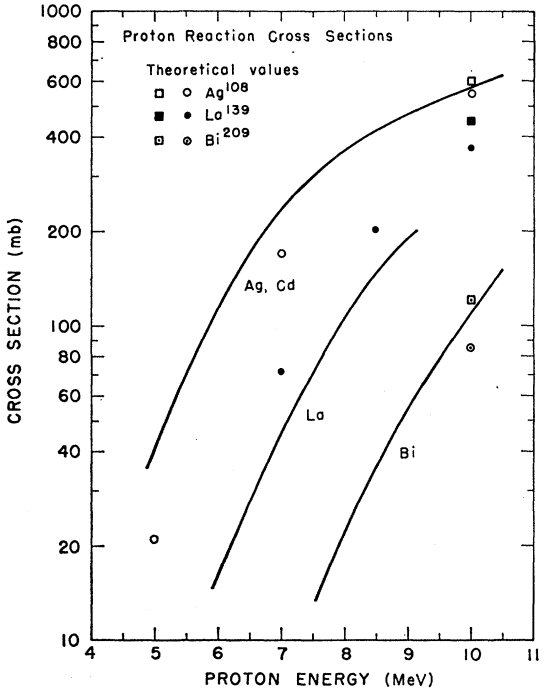

FIG. 13. Proton reaction cross sections of Ag, Cd, La, and Bi. Solid curves represent experimental-reaction cross sections determined by method 1. Open points designate the theoretical-reaction cross sections for Ag^{108}, solid points the theoretical-reaction cross sections for La^{139}, and ⊡ and ⊙ the theoretical-reaction cross sections for Bi^{209}. Squares are surface adsorption (references 2, 29) and circles are volume absorption with $r_0=1.25$ F, and $d=0.52$ F. For Ag and Bi, $V=-62$ MeV and $W=-8.6$ MeV. For La, $V=-55$ MeV and $W=-6$ MeV.

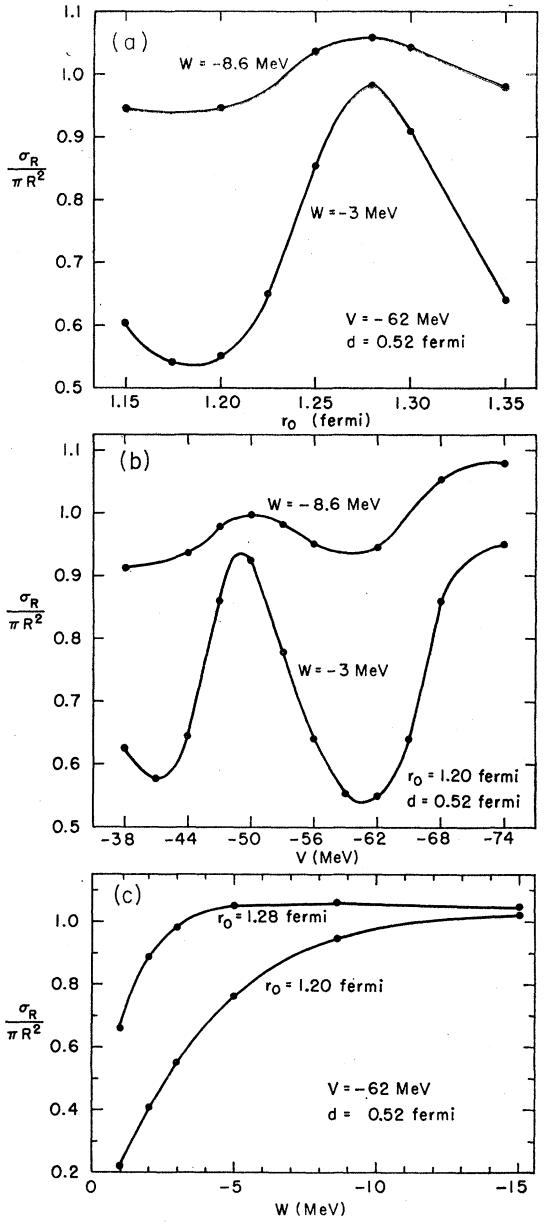

FIG. 14. Theoretical reaction cross section divided by πR^2, where $R=r_0A^{\frac{1}{3}}$, for 10-MeV protons on Cu^{64}. The two sets of Woods-Saxon parameters found in reference 27 are $V=-62$ MeV, $W=-8.6$ MeV, $r_0=1.20$ F, and $d=0.52$ F; and $V=-48$ MeV, $W=-7.9$ MeV, $r_0=1.33$ F, and $d=0.50$ F.

of the parameters V, W, r_0, a, and b of $-[44+(Z/A^{\frac{1}{3}})]$ MeV, -11 MeV, 1.25 F, 0.65 F, and 1.2 F, respectively, and a spin-orbit potential of 20 times the Thomas term. All of the surface absorption cross sections at 10 MeV which are discussed in this paper are based on these parameters.

Optical model calculations with surface absorption[2,29] give 10-MeV proton cross sections of 805 and

[28] J. S. Nodvik and D. S. Saxon, Phys. Rev. **117**, 1539 (1960).

[29] F. Bjorklund and S. Fernbach, Phys. Rev. **109**, 1295 (1958).

850 mb for copper and vanadium, respectively. The experimental total reaction cross sections of Cu^{63} and Cu^{65} with 10-MeV protons agree slightly better with surface absorption than with volume absorption optical-model calculations, although surface absorption does not[7] give better agreement with experiment with 7.5-MeV protons. The experimental reaction cross section of 800 mb for vanadium with 10-MeV protons does not include the (p,p') cross section[1] to the 0.32- and 0.65-MeV states in V^{51}, and hence is a lower limit. Calculations with both surface and volume absorption[7] agree with the experimental vanadium cross section with 7.5-MeV protons.

A volume absorption optical model calculation with $r_0=1.25$ F gives reaction cross sections for silver, cadmium, lanthanum, and bismuth which are in reasonable agreement with the experimental-reaction cross sections. This conclusion is rather tentative since the range of Woods-Saxon parameters which fit the elastic scattering have not been established. The surface [2,29] absorption model gives a 10-MeV cross section of about 600 mb for silver and cadmium, 450 mb for lanthanum, and 120 mb for bismuth. The theoretical cross sections calculated with both volume and surface absorption are compared with the experimental results in Fig. 13. As can be seen from Fig. 13, the experimental cross sections of lanthanum are low compared to the calculated values. The experimental cross sections of lanthanum are, however, slightly larger than the cross sections reported for praseodymium.[4] For both of the latter two targets, the (p,n) cross sections should be reasonable approximations of the total-reaction cross sections for energies less than the threshold of the $(p,2n)$ reaction which occurs at about 8.5 MeV for both targets.

ACKNOWLEDGMENTS

The authors are indebted to M. C. Oselka for performing the cyclotron bombardments, F. J. Karasek for the preparation of the thin metallic foils, D. J. Henderson for assistance in sample counting, E. G. Rauh for the preparation of the lanthanum and bismuth targets, and J. P. Faris and R. W. Bane for a quantitative assay of the lanthanum and bismuth targets, respectively. We also wish to thank J. P. Schiffer for helpful discussions.